



HAL
open science

Improving the genistein oral bioavailability via its formulation into the metal–organic framework MIL-100(Fe)

Adrià Botet-Carreras, Cristina Tamames-Tabar, Fabrice Salles, Sara Rojas,
Edurne Imbuluzqueta, Hugo Lana, María José Blanco-Prieto, Patricia
Horcajada

► To cite this version:

Adrià Botet-Carreras, Cristina Tamames-Tabar, Fabrice Salles, Sara Rojas, Edurne Imbuluzqueta, et al.. Improving the genistein oral bioavailability via its formulation into the metal–organic framework MIL-100(Fe). *Journal of materials chemistry B*, 2021, 9 (9), pp.2233-2239. 10.1039/D0TB02804E . hal-03168325

HAL Id: hal-03168325

<https://hal.science/hal-03168325>

Submitted on 30 Apr 2021

HAL is a multi-disciplinary open access archive for the deposit and dissemination of scientific research documents, whether they are published or not. The documents may come from teaching and research institutions in France or abroad, or from public or private research centers.

L'archive ouverte pluridisciplinaire **HAL**, est destinée au dépôt et à la diffusion de documents scientifiques de niveau recherche, publiés ou non, émanant des établissements d'enseignement et de recherche français ou étrangers, des laboratoires publics ou privés.

Improving the Genistein oral bioavailability by its formulation into the Metal-Organic Framework MIL-100(Fe)

Adrià Botet-Carreras,^{a,b,#} Cristina Tamames-Tabar,^{a,b,#} Fabrice Salles,^c Sara Rojas,^d Edurne Imbuluzqueta,^a Hugo Lana,^a María José Blanco-Prieto,^{a,*} Patricia Horcajada^{b,d,*}

Despite the interesting chemopreventive, antioxidant and antiangiogenic effects of the natural bioflavonoid genistein (GEN), its low aqueous solubility and bioavailability make it necessary to administer it using a suitable drug carrier system. Nanometric porous Metal-Organic Frameworks (nanoMOFs) are appealing systems for drug delivery. Particularly, the mesoporous MIL-100(Fe) possesses a variety of interesting features related to its composition and structure, which make it an excellent candidate to be used as a drug nanocarrier (highly porous, biocompatible, can be synthesized as homogenous and stable nanoparticles (NPs), etc.). In this study, GEN was entrapped by simple impregnation in MIL-100 NPs achieving a remarkable drug loading (27.1 wt%). A combination of experimental and computing techniques was used to achieve a deep understanding of the encapsulation of GEN in MIL-100 nanoMOF. Subsequently, GEN delivery studies were carried out under simulated physiological conditions, showing on the whole a sustained GEN release for 3 days. Initial pharmacokinetics and biodistribution studies were also carried out upon the oral administration of the GEN@MIL-100 NPs in a mouse model, evidencing a higher bioavailability and showing that this oral nanoformulation appears very promising. To the best of our knowledge, the GEN-loaded MIL-100 will be the first antitumor oral formulation based on nanoMOFs studied *in vivo*, and paves the way to efficiently deliver nontoxic antitumorals by a convenient oral route.

Introduction

Nowadays, we are increasingly returning to nature in matters regarding nutrition and therapeutics. Bioflavonoids or phytoestrogens are in vogue. Particularly, the bioflavonoid genistein (GEN), which is found in many fruits, vegetables, legumes and plant leaves, has a wide array of compelling applications in therapeutics.¹² Among them, probably the best-known activity of GEN is as a chemopreventive and anticancer agent.³ In sharp contrast with some cytotoxic drugs currently used, GEN's oral consumption presents a moderate toxicity (with an oral median lethal dose-LD₅₀ in mouse of 500 mg·Kg⁻¹ vsLD₅₀ cisplatin = 14.5 mg·Kg⁻¹, 5-fluorouracil = 230 mg·Kg⁻¹, LD₅₀ dactinomycin = 13mg·Kg⁻¹) due to its different action mechanism based on the alterations that this natural product causes in the cell cycle (*i.e.*, apoptosis or inhibition of cell proliferation, by inhibition of topoisomerase II,⁴ by blockage of protein tyrosine kinase,⁵ or by bringing about alterations in the phosphatidylinositol turnover). In this sense, the reported half maximal inhibitory concentration-IC₅₀ of GEN is 0.27, 0.54, 10.5, and 6.5 μg·mL⁻¹ in human myoblastic leukemia-MLI, human gastric cancer, human breast carcinoma cell lines MCG-7, and MDA-468 cells, respectively.⁶⁻⁸ In the last few years, several studies have shown its benign effect in leukaemia,⁵ breast cancer,⁹ and prostate cancer,¹⁰ as well as in metastasis.¹¹ In addition, GEN inhibits the production of reactive oxygen species,⁵ blocks multidrug resistance proteins,¹² suppresses bone degradation and decreases cardiovascular-related diseases.¹³ Finally, it could also be useful for the treatment of cystic fibrosis,¹⁴ allergic processes,¹⁵ obesity,¹⁶ skin photoaging,¹⁷ and as a neuroprotective agent.¹⁸

Despite all the promising properties GEN possesses, several important drawbacks that limit its clinical use, including its very low water solubility and low bioavailability (F). Its low F is

mainly related to: *i*) an important first-pass metabolism and enterohepatic recycling,¹⁹ *ii*) high serum protein binding,²⁰ *iii*) low absorption when orally administered (notwithstanding, aglycones are more rapidly absorbed when contrasted to glycones, a role connected to the sugar moiety),²¹ and *iv*) the effect of efflux proteins, which prevent blood absorption of GEN.²² Rationally, the encapsulation of GEN should be able to overcome the previously described drawbacks, achieving a secure and effective drug dosage form.

In recent years, GEN has been loaded in different polymeric formulations²³ (9 wt% in d- α -tocopheryl polyethylene glycol

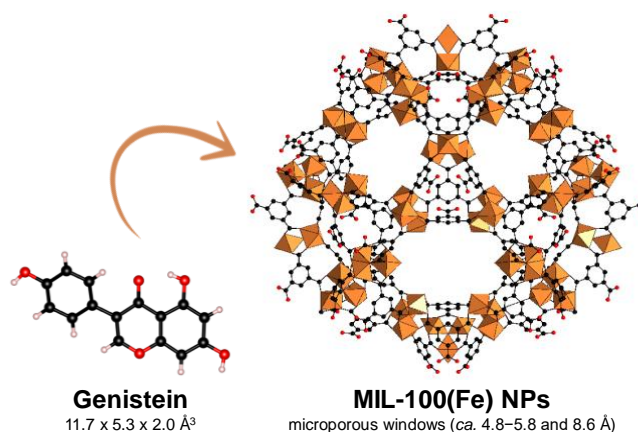


Figure 1. Schematic view of the large cavity of the MIL-100 structure (iron polyhedra, oxygen, and carbon are represented in orange, red and black, respectively; hydrogen atoms are omitted for clarity). Chemical structure of genistein drug is also given.

1000 succinate (TPGS),¹ 10 wt% in M-PLGA-TPGS (PLGA = poly(D,L-lactide-co-glycolide)),²⁴ 4 wt% in PVA@SiO₂ (PVA = polyvinyl alcohol),²⁵ 14 wt% in PEGylated silica (PEG = polyethylene glycol),²⁶ or 7.3 wt% in lipid nanoparticles (NPs),²⁷ achieving drug loadings up to 14.5 μg of GEN *per* mg of formulation. Metal-organic frameworks (MOFs) are a specific

type of crystalline hybrid solids, built up from the assembly of inorganic secondary building units and easily tuneable polycomplexant organic linkers, exhibiting exceptional porosities.^{28,29} Particularly, their miniaturization results in nanometric MOFs (nanoMOFs), combining the intrinsic properties of the porous materials and the benefits of nanostructures, strongly interesting in the biomedical field.^{30,31} MOFs have been proposed for the encapsulation and delivery of several active ingredients (drugs,^{30,32} cosmetics,^{33,34} biologically active gases,³⁵ enzymes,³⁶ and toxins,³⁷ and imaging agents in theranostic).³⁸ The vast majority of the investigations dealing with the use of MOFs as drug delivery platforms are focused on the intravenous route. The simple, accessible and convenient oral route using MOFs as drug carriers is reduced to two examples (the administration of the antigen ovalbumin with an Al-based MOF,³⁹ and the administration of the neuroactive magnolol through the UiO-66 framework).⁴⁰ In the present study we selected one of the most promising MOF nanocarriers, the benchmarked mesoporous MIL-100(Fe) NPs or $[\text{Fe}_3\text{O}(\text{H}_2\text{O})_2\text{OH}(\text{BTC})_2] \cdot n\text{H}_2\text{O}$ ($\text{H}_3\text{BTC} = 1,3,5\text{-benzenetricarboxylic acid}$ or trimesic acid), which possesses a variety of interesting features:⁴¹ *i*) it is highly porous (Brunauer, Emmett and Tellet (BET) surface area $\sim 2000 \text{ m}^2 \cdot \text{g}^{-1}$, $V_p \sim 1.2 \text{ cm}^3 \cdot \text{g}^{-1}$) and shows mesoporous voids of 2.5 and 2.9 nm, accessible through microporous windows (*ca.* 4.8–5.8 and 8.6 Å, respectively), compatible with GEN dimensions ($12 \times 5 \times 2 \text{ \AA}^3$, **Figure 1**); *ii*) it can be prepared as homogeneous and stable NPs (*ca.* 140 nm) with an optimal colloidal stability in different physiological media;⁴² *iii*) it is a nontoxic and biodegradable material,^{42,43} built up from nontoxic components (Fe(III) and H_3BTC , the oral media lethal dose- LD_{50} in rats for FeCl_3 and H_3BTC is 450 and 8400 $\text{mg} \cdot \text{Kg}^{-1}$, respectively), having proven no sign of toxicity against different cell lines (*e.g.*, HeLa, J774).⁴⁴ Furthermore, after its intravenous administration ($220 \text{ mg} \cdot \text{kg}^{-1}$) in rats, this material has been demonstrated to be biocompatible, biodegradable (without metabolization), and bioremovable by feces and urines,⁴⁵ and *iv*) it can be coated with different macromolecules in order to modify its intestinal permeation and biodistribution (*e.g.*, long-circulating NPs).^{46,47} Taking into account these characteristics, we report here a GEN oral formulation using MIL-100 NPs. We studied in detail the GEN encapsulation in MIL-100 NPs using experimental and computational techniques, evaluating the efficiency of the resulting formulation *in vitro*. Then, we investigated its pharmacokinetic and biodistribution *in vivo* upon the oral administration of the formulation to a mouse model. To the best of our knowledge, the GEN-loaded MIL-100 will be the first antitumor oral formulation based on nanoMOFs studied *in vivo* so far.

Results and discussion

GEN encapsulation

The GEN encapsulation was performed by simple impregnation, suspending the MIL-100 NPs into a concentrated aqueous solution of GEN. The GEN loading was quantified by the combination of thermogravimetric analysis (TGA), elemental analysis, and high-performance liquid chromatography (HPLC, see **Supporting Information, Section 2**). A sizeable GEN loading was achieved ($271 \pm 34 \text{ mg} \cdot \text{g}^{-1}$ or 27.1 wt% expressed as the wt% of GEN over the formulation). This value is in total agreement with the encapsulation rates obtained for MIL-100 NPs and other drugs (*i.e.*, 24 wt% of azidothymidine triphosphate,⁴⁸ 25 wt% of busulfan,⁴⁹ 16.1 wt% of cidofovir, 9.1 wt% of doxorubicin, 33 wt% of ibuprofen, 24.2 wt% of caffeine,⁴¹ and 29.6 wt% of RAPTA-C).⁵⁰ Although studies dealing with GEN encapsulation are still scarce, these encapsulation rates are higher than those previously reported using different drug carriers, such as polymeric²³ (*i.e.*, 9 wt% in TPGS,¹ 10 wt% in M-PLGA-TPGS,²⁴ 4 wt% in PVA@ SiO_2 ,²⁵ 14 wt% in PEGylated silica),²⁶ or 7.3 wt% in lipid NPs.²⁷ The GEN loading rate in MIL-100 NPs is even higher when considering the lower density of the polymer/lipid NPs compared with hybrid nanoMOFs. Therefore, the GEN-nanoMIL-100 formulation seems to be very promising for GEN administration.

However, to reach these important encapsulation rates, the GEN encapsulation was optimized by modifying some different parameters (solvent, GEN source, encapsulation temperature). First, ethanol (EtOH) and dichloromethane (DCM) were selected due to the high GEN experimental solubility (~ 1.3 and $2.0 \text{ mg} \cdot \text{mL}^{-1}$, respectively), their low toxicity values (LD_{50} in rats = 7060 and 2100 $\text{mg} \cdot \text{Kg}^{-1}$, respectively),⁵¹ and their easy removal at low temperature ($<80 \text{ }^\circ\text{C}$; **Supporting Information, Table S1**). Lower encapsulation rates when using an EtOH and DCM solution were obtained ($\sim 18 \text{ } \mu\text{g} \cdot \text{mg}^{-1}$), followed with the presence of free recrystallized GEN in the case of DCM encapsulation, as observed by powder X-ray powder diffraction (PXRD). In the case of EtOH, it is known that it can bind the coordinatively unsaturated iron(III) metal sites (CUS) pointing to the center of the window, then considerably decreasing the free diameter or the hexagonal (from 8.2 to 4.1 Å) and pentagonal (from 4.5 to 1.7 Å) windows, and therefore, drastically reducing the diffusion of GEN into the pores, particularly into the smaller cages.⁵²

Therefore, a new strategy was developed to improve GEN loading in MIL-100 NPs. A dicalcium salt of GEN (denoted as GCa) was prepared in order to increase its water solubility (from 0.0008 to $1.4 \text{ mg} \cdot \text{mL}^{-1}$, **Supporting Information, Table S1**), allowing the use of bio-friendly and low-cost aqueous solutions for GEN encapsulation.

Table 1. GEN loadings together with the BET surface (S_{BET}) and micropore volume (V_p) for MIL-100 NPs and the GEN loaded GEN@MIL-100 NPs.

Material	GEN loading $\text{mg}\cdot\text{g}^{-1}$ ($\text{mol}\cdot\text{mol}^{-1}$)		Textural properties	
	Experimental	Theoretical	V_p ($\text{cm}^3\cdot\text{g}^{-1}$)	SBET ($\text{m}^2\cdot\text{g}^{-1}$)
MIL-100 NPs	-	-	0.66	1460
GEN@MIL-100 NPs	271 ± 34 (0.71)	456^{a} 236^{b}	0.01	30

^{a)} theoretical value estimated by Monte Carlo simulation, ^{b)} blocking the access to the small cavities of MIL-100 NPs (see **Section 4**).

Interestingly, higher encapsulation rates were achieved using GCa aqueous solutions at moderate temperature (271 vs. $18 \mu\text{g mg}^{-1}$ for GCa in water at 37°C , and GEN in EtOH at room temperature (RT), respectively), as the drug diffusion throughout the MIL-100 NPs porosity was directly related to the temperature. In addition, elemental analysis measurements showed the presence of a small amount of calcium. Considering that *i)* the pH of the encapsulation medium was 6.6 (associated with the presence of partially coordinated trimesate linkers located on the outer surface of MIL-100 NPs), and *ii)* the presence of hydroxyl groups in the GEN molecule ($\text{pK}_{\text{a}1} = 7.2$, $\text{pK}_{\text{a}2} = 10.0$, and $\text{pK}_{\text{a}3} = 13.1$),⁵³ this value might correspond to *ca.* 6% of the total encapsulated GEN entrapped as monocalcium form in the MIL-100(Fe) NPs. Although in a small proportion, the presence of a GEN salt could improve the GEN bioavailability due to the improved aqueous solubility of this fraction.

The incorporation of GEN into the MIL-100 cavities was further demonstrated by *i)* the dramatic reduction in the N_2 sorption capacity of the MOF at 77 K , *ii)* the presence of some characteristic peaks of the pure GEN in the Fourier transform infrared (FTIR) spectrum of GEN@MIL-100 NPs, and *iii)* the differences found in thermal stability of the GEN@MIL-100 NPs and the pristine material (**Table 1**, **Supporting Information, Figure S1**). Further, both structural and colloidal features of the MIL-100 NPs were kept intact after the GEN encapsulation negatively charged NPs of *ca.* -25 mV with dimensions of 129 ± 26 and $161 \pm 46\text{ nm}$ before and after encapsulation, respectively, **Supporting Information, Table S3**).

In order to check if the maximum theoretical GEN loading had been experimentally achieved, force-field-based Grand Canonical Monte Carlo (GCMC) simulations were employed (see **Supporting Information, Section 3**). The experimental GEN cargoes were much lower than the theoretical ones (271 vs. $456\text{ mg}\cdot\text{g}^{-1}$). These differences might be due to not considering the coadsorption of the encapsulation solvent during the GEN entrapping, something that happens experimentally. Hence, we presume that theoretical uptake was probably overestimating the saturation. Further, the theoretical loading was estimated by assuming a full accessibility of both small and large cages. However, considering that the dimensions of GEN ($11.7 \times 5.3 \times 2.0\text{ \AA}^3$) are quite close to the window size of the small cage ($\sim 4.7 \times 5.5\text{ \AA}^2$), one can rationally expect that only the large cages (8.6 \AA)

will be accessible to GEN adsorption. Thus, blocking the volume of the small cages (54%), we can roughly estimate an encapsulation rate of $236\text{ mg}\cdot\text{g}^{-1}$ (corresponding to 54 GEN molecules *per* cage), which is in good agreement with the experimental payload ($271 \pm 34\text{ mg}\cdot\text{g}^{-1}$).

The formation of specific interaction was also investigated by GCMC simulation and FTIR. From these calculations, the GEN conformation inside the pores was estimated, evidencing that the main interactions between the nanoMOF and the GEN correspond to π -stacking interactions between the aromatic ring of the GEN moieties and the trimesate of the MIL-100 NPs (**Figure 2**). In agreement with GCMC calculations, FTIR showed a shift of $\nu/\delta(\text{C}=\text{C})$ bands at around 1500 cm^{-1} , which could be in accordance with the formation of π -interactions (**Supporting Information, Figure S1c**).

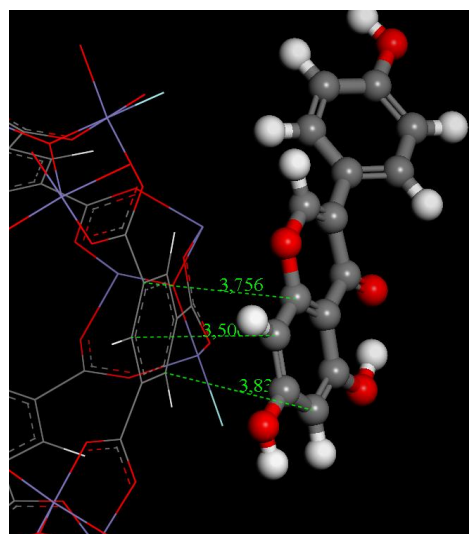


Figure 2. GCMC structures of MIL-100 NPs in presence of GEN. Characteristic GEN/MOF interacting distances are reported in Angstrom (in green).

GEN release under physiological oral conditions

GEN release was firstly evaluated under simulated intestinal conditions by suspending the GEN@MIL-100 NPs in a phosphate buffer saline solution (PBS, 0.04 M at $\text{pH} = 7.2$) at 37°C under continuous stirring. The released GEN was quantified by HPLC. In parallel, to assess the potential MOF structural degradation under the release conditions, the delivery of the constitutive organic linker was monitored also by HPLC.

The complete release of GEN was reached after 3 days under simulated intestinal conditions (**Figure 3**), with two different

steps: a burst release of GEN in the first 30 min (~ 40%) followed by a progressive delivery within 3 days. The first initial fast release is likely due to the open character of the MIL-100 structure, with large interconnected cavities. Apart from the effect of the open character of the MOF and the drug/medium diffusion, controlled released of GEN from the MIL-100 NPs might be associated with *i*) the formation of specific host-guest interactions between the drug and the MOF (demonstrated by GCMC and FTIR), *ii*) the slow diffusion of the GEN through the pores due to its hydrophobic character ($\log P = 3.04$),⁵⁴ *iii*) and the MOF degradation under physiological conditions.⁵⁵ Interestingly, the degradation rate seems to fit rather well with the GEN release profile (**Supporting Information, Figure S2**), indicating that the MOF chemical degradation is an important parameter affecting the GEN release.

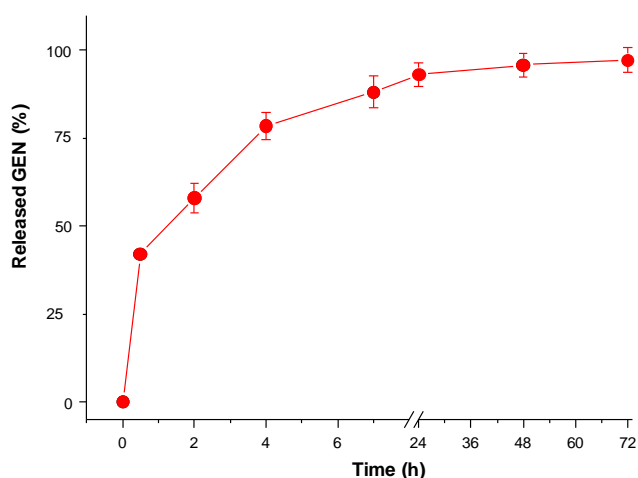


Figure 3. GEN release over 3 days from MIL-100 NPs under simulated intestinal conditions. Note that lines are only visual guides.

In vivo GEN release under oral conditions

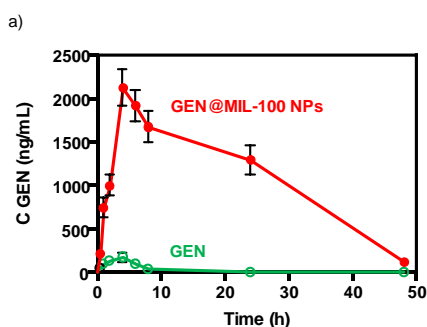
GEN@MIL-100 NPs show some interesting properties for their use as drug delivery systems since: *i*) they can be prepared as monodispersed NPs under totally biofriendly conditions (aqueous solvent) with very important reaction yield (87%); *ii*)

they show a good GEN encapsulation rate ($271 \text{ mg}\cdot\text{g}^{-1}$), higher than those reported using other nanocarriers; *iii*) while keeping the nanometric size; and *iv*) they are able to progressively release GEN over 3 days under simulated physiological intestinal conditions. However, prior to their clinical use, a series of preclinical studies need to be carried out (see **Supporting Information, Section 5** for further details).

Pharmacokinetics

The release of GEN from MIL-100 NPs was finally evaluated *in vivo*. To the best of our knowledge, no other examples of flavonoid antitumor oral formulations based on nanoMOF has been investigated *in vivo* so far. We orally administered $30 \text{ mg}\cdot\text{Kg}^{-1}$ of free GEN or GEN@MIL-100(Fe) NPs (**Figure 4**). Interestingly, there are significant differences in GEN plasma levels between encapsulated and free GEN. The maximum concentration (T_{\max}) was reached 4 h post-administration in both free and encapsulated GEN, with maximal drug concentration values (C_{\max}) of 171.25 and $2123.29 \text{ ng}\cdot\text{mL}^{-1}$, respectively. Moreover, 8 h post-administration, a reduction in GEN levels was observed in both groups, being more pronounced in the case of the encapsulated drug (36.47 and $1643.88 \text{ ng}\cdot\text{mL}^{-1}$ for free and encapsulated GEN, respectively). It should be highlighted that after 24 and 48 h, there were still some plasmatic levels of GEN when the GEN@MIL-100 NPs formulation was administered (1292.85 and $120.07 \text{ ng}\cdot\text{mL}^{-1}$ for 24 and 48 h, respectively), while in the case of free GEN no drug was detected. From the slow release (3 days) of GEN under simulated intestinal conditions, one could suggest that the active cargo is retained in the MOF as far as the target intestine. Even considering that the MOF carrier is not absorbed, the progressive and localized GEN release close to the intestinal membrane might favor its intestinal absorption, leading to higher plasmatic concentration. The plasma concentration in the case of free GEN here presented is in agreement with that observed by King and Bursill, in which GEN was quickly eliminated from plasma, dropping to residual levels 12-24 h after a soy meal consumption, evidencing a short half-life ($t_{1/2}$).⁵⁶

Interestingly, the administration of our formulation increased by 12-fold the drug plasmatic levels (~ 170 vs. $\sim 2100 \text{ ng}\cdot\text{mL}^{-1}$



b)

PK parameters	Free GEN	Encaps. GEN
C_{\max} ($\text{ng}\cdot\text{mL}^{-1}$)	171.25	2123.29
T_{\max} (h)	4	4
$t_{1/2}$ (h)	1.79	10.12
MRT (h)	3.82	16.23
F_{rel} ($\text{ng}\cdot\text{h}\cdot\text{mL}^{-1}$)	900	52600
F_{abs} (%)	-	+25%

Figure 4. a) Time-plasma concentration curve data of GEN (green, empty circles) and GEN@MIL-100 NPs (red, filled circles) after a single oral administration of $30 \text{ mg}\cdot\text{Kg}^{-1}$ ($n = 6$) during 48 h. b) Pharmacokinetics parameters obtained with WinNonLin[®] software. F_{abs} obtained from reference.⁵⁷

for free and encapsulated GEN, respectively), incremented 4-fold the mean residence time (MRT, 3.82 vs. 16.23 h for free and encapsulated GEN, respectively) and raised 5.5-fold the drug half-life ($t_{1/2}$, 1.79 vs. 10.12 h for free and encapsulated GEN, respectively). Most importantly, the loading of GEN in the MIL-100 NPs enhanced the relative bioavailability (F) 62-fold (area under the curve-AUC \sim 900 vs. \sim 52600 ng·h·mL⁻¹ for both free and encapsulated GEN, respectively), as well as the absolute F by \sim 25% when compared with free GEN intravenously administered (AUC \sim 52600 vs. \sim 212000 ng·h·mL⁻¹, respectively).⁵⁷ Aside from the increased drug saturation in GEN@MIL-100 NPs by the formation of the calcium salt of GEN, the probable adherence of the GEN@MIL-100 NPs to the intestinal mucosa (as previously observed in MIL-127 MOF)⁵⁸ will favor the local GEN release, leading to highly concentrated areas near to the mucosa and thus increasing the drug availability. At this point, our results could be referred to other promising GEN formulations based on different carriers (polymeric micelles or lipid nanoparticles). Our MOF-based nanoformulation presents similar or even improved pharmacokinetic parameters (AUC = 52600 ng·h·mL⁻¹, C_{max} = 2123 ng·mL⁻¹, $t_{1/2}$ = 10.1 h) when compared to previously reported nanoformulations (e.g., AUC = 99500 ng·h·mL⁻¹, C_{max} = 16000 ng·mL⁻¹, $t_{1/2}$ = 7.5 h for intravenous administered polyethylenglycol modified copolymer micelles (MePEG-PLGA),⁵⁹ and AUC = 7500 ng·h·mL⁻¹, C_{max} = 1200 ng·mL⁻¹, $t_{1/2}$ = 5.9 h for orally administered GEN-loaded solid lipid nanoparticles).⁶⁰ Note here that a direct comparison is hindered by the different conditions in the studies.

GEN biodistribution

In a preliminary study, we quantified the amount of GEN in some organs (i.e., liver, kidneys, and spleen) for both formulations (free GEN and GEN@MIL-100 NPs) 8 hours after the administration, when the T_{max} was already achieved. Note that GEN was only measurable in liver, where its amount was doubled in the free GEN group when compared with the GEN@MIL-100 NPs group (1.4 ± 1.3 vs. 0.6 ± 0.3 μ g·g⁻¹, corresponding to ca. 0.06 to 0.09% of the initial dose, respectively). Regarding the amount of GEN in spleen, it was under the limit of detection (LOD) in the GEN@MIL-100 NPs group and under the limit of quantification (LOQ) in the free GEN group, while in the kidneys GEN was under the LOD in both groups. All these data support the notion that the GEN is protected from metabolism *via* its encapsulation inside MIL-100 porosity, and therefore, was detected for a longer time when compared to the free drug formulation.

Conclusions

In this study, we report a reproducible GEN@MIL-100 NPs formulation with an adsorbed amount of GEN of 271 ± 34 mg·g⁻¹ surpassing the GEN loading achieved with other GEN formulations. Further, the GEN exhibited a progressive release profile that persists for 3 days, being likely related to the open character of the framework and its degradation in PBS. After the oral administration of GEN@MIL-100 formulation to mice, longer time and higher plasmatic levels were observed, with a

higher oral bioavailability when compared with the free drug. Moreover, on the basis of the first preliminary biodistribution tests, we can say that the MOF seems to act as a shelter for GEN, impeding its metabolism. These results pave the way to efficiently deliver the nontoxic antitumor GEN by a convenient oral route avoiding the main drawbacks (low solubility and bioavailability) associated with its important metabolism and poor oral absorption when administered free.

Conflicts of interest

There are no conflicts to declare.

Acknowledgements

Authors thank the technical support of F. Ragon for MOF synthesis guidance and M. A. Campanero for HPLC assessment. Authors would like to acknowledge Asociación de Amigos de la Universidad de Navarra for the predoctoral grant of C.T-T. A.B-C. Thanks to the Labex NanoSaclay for the MSc financial support (ANR-11-IDEX-0003-02). This work was partially supported by FeUN (Fundación Empresa Universidad de Navarra), University of Versailles Saint Quentin-en-Yvelines, and CNRS funding. S.R. and P.H. acknowledge the regional Madrid founding (Talento 2017 Modality 2, 2017-T2/IND-5149), the MOFSEIDON project (PID2019-104228RB-I00, MCI/AEI/FEDER, UE), and the Multifunctional Metallodrugs in Diagnosis and Therapy Network (MICIU, RED2018-102471-T). PH acknowledges the Spanish Ramon y Cajal Programme (grant agreement no. 2014-16823). S.R. acknowledges the Spanish Juan de la Cierva Incorporación Fellowship (grant agreement no. IJC2019-038894-I).

Notes and references

- 1 H. Zhang, G. Liu, X. Zeng, Y. Wu, C. Yang, L. Mei, Z. Wang and L. Huang, *Int. J. Nanomedicine*, 2015, **10**, 2461–2473.
- 2 K. Polkowski and A. P. Mazurek, *Acta Pol. Pharm. - Drug Res.*, 2000, **57**, 135–155.
- 3 F. H. Sarkar and Y. Li, *Cancer Res.*, 2006, **66**, 3347–3350.
- 4 A. M. Azarova, R. K. Lin, Y. C. Tsai, L. F. Liu, C. P. Lin and Y. L. Lyu, *Biochem. Biophys. Res. Commun.*, 2010, **399**, 66–71.
- 5 Y. Sánchez, C. Calle, E. de Blas and P. Aller, *Chem. Biol. Interact.*, 2009, **182**, 37–44.
- 6 M. Makishima, Y. Honma, M. Hozumi, K. Sampi, M. Hattori, K. Umezawa and K. Motoyoshi, *Leuk. Res.*, 1991, **15**, 701–708.
- 7 S. Barnes, *J. Nutr.*, 1995, **125**, 777S.
- 8 G. Peterson and S. Barnes, *Biochem. Biophys. Res. Commun.*, 1991, **179**, 661–667.
- 9 R. Banerjee, A. Phan, B. Wang, C. Knobler, H. Furukawa, M. O’Keeffe and O. M. Yaghi, *Science*, 2008, **319**, 939–943.
- 10 S. Banerjee, Y. Li, Z. Wang and F. H. Sarkar, *Cancer Lett.*, 2008, **269**, 226–242.
- 11 J. M. Pavese, R. L. Farmer and R. C. Bergan, *Cancer Metastasis Rev.*, 2010, **29**, 465–482.
- 12 A. F. Castro and G. A. Altenberg, *Biochem. Pharmacol.*,

- 1997, **53**, 89–93.
- 13 L. G. Ming, K. M. Chen and C. J. Xian, *J. Cell. Physiol.*, 2013, **228**, 513–521.
- 14 K. A. Lansdell, Z. Cai, J. F. Kidd and D. N. Sheppard, *J. Physiol.*, 2000, **524**, 317–330.
- 15 E. Brzezińska-Błaszczczyk, A. Pietrzak and A. H. Misiak-
Tłoczek, *J. Interf. Cytokine Res.*, 2007, **27**, 911–919.
- 16 N. Behloul and G. Wu, *Eur. J. Pharmacol.*, 2013, **698**, 31–
38.
- 17 F. Polito, H. Marini, A. Bitto, N. Irrera, M. Vaccaro, E. B.
Adamo, A. Micali, F. Squadrito, L. Minutoli and D. Altavilla,
Br. J. Pharmacol., 2012, **165**, 994–1005.
- 18 W. Liao, G. Jin, M. Zhao and H. Yang, *Basic Clin. Pharmacol.*
Toxicol., 2013, **112**, 182–185.
- 19 S. Kobayashi, M. Shinohara, T. Nagai and Y. Konishi, *Biosci.*
Biotechnol. Biochem., 2013, **77**, 2210–2217.
- 20 A. Bolli, M. Marino, G. Rimbach, G. Fanali, M. Fasano and P.
Ascenzi, *Biochem. Biophys. Res. Commun.*, 2010, **398**, 444–
449.
- 21 K. D. R. Setchell, N. M. Brown, P. Desai, L. Zimmer-
Nechemias, B. E. Wolfe, W. T. Brashear, A. S. Kirschner, A.
Cassidy and J. E. Heubi, *J. Nutr.*, 2001, **131**, 1362S-1375S.
- 22 L. M. S. Chan, S. Lowes and B. H. Hirst, *Eur. J. Pharm. Sci.*,
2004, **21**, 25–51.
- 23 N. Tyagi, Y. H. Song and R. De, *J. Drug Target.*, 2019, **27**,
394–407.
- 24 B. Wu, Y. Liang, Y. Tan, C. Xie, J. Shen, M. Zhang, X. Liu, L.
Yang, F. Zhang, L. Liu, S. Cai, D. Huai, D. Zheng, R. Zhang, C.
Zhang, K. Chen, X. Tang and X. Sui, *Mater. Sci. Eng. C*, 2016,
59, 792–800.
- 25 Y. Zhang, B. Gao and Z. Xu, *J. Phys. Chem. B*, 2013, **117**,
5730–5736.
- 26 H. Pool, R. Campos-Vega, M. G. Herrera-Hernández, P.
García-Solis, T. García-Gasca, I. C. Sánchez, G. Luna-
Bárceñas and H. Vergara-Castañeda, *Am. J. Transl. Res.*,
2018, **10**, 2306–2323.
- 27 J. Pham, B. Brownlow and T. Elbayoumi, *Mol. Pharm.*,
2013, **10**, 3789–3800.
- 28 H. C. Zhou, J. R. Long and O. M. Yaghi, *Chem. Rev.*, 2012,
112, 673–674.
- 29 H. C. J. Zhou and S. Kitagawa, *Chem. Soc. Rev.*, 2014, **43**,
5415–5418.
- 30 M. Giménez-Marqués, T. Hidalgo, C. Serre and P.
Horcajada, *Coord. Chem. Rev.*, 2015, **307**, 342–360.
- 31 P. Horcajada, R. Gref, T. Baati, P. K. Allan, G. Maurin and P.
Couvreur, in *Metal-Organic Frameworks: Applications from*
Catalysis to Gas Storage, 2012, pp. 1232–1268.
- 32 S. Rojas, A. Arenas-Vivo and P. Horcajada, *Coord. Chem.*
Rev., 2019, **388**, 22–226.
- 33 D. Cunha, M. Ben Yahia, S. Hall, S. R. Miller, H. Chevreau, E.
Elkaïm, G. Maurin, P. Horcajada and C. Serre, *Chem.*
Mater., 2013, **25**, 2767–2776.
- 34 N. Liédana, A. Galve, C. Rubio, C. Téllez and J. Coronas, *ACS*
Appl. Mater. Interfaces, 2012, **4**, 5016–5021.
- 35 S. Rojas, P. S. Wheatley, E. Quartapelle-Procopio, B. Gil, B.
Marszalek, R. E. Morris and E. Barea, *CrystEngComm*, 2013,
15, 9364–9367.
- 36 V. Lykourinou, Y. Chen, X. Sen Wang, L. Meng, T. Hoang, L.
J. Ming, R. L. Musselman and S. Ma, *J. Am. Chem. Soc.*,
2011, **133**, 10382–10385.
- 37 C. A. F. de Oliveira, F. F. da Silva, G. C. Jimenez, J. F. da S.
Neto, D. M. B. de Souza, I. A. de Souza and S. A. Junior,
Chem. Commun., 2013, **49**, 6486–6488.
- 38 H. S. Wang, *Coord. Chem. Rev.*, 2017, **349**, 139–155.
- 39 Y. B. Miao, W. Y. Pan, K. H. Chen, H. J. Wei, F. L. Mi, M. Y.
Lu, Y. Chang and H. W. Sung, *Adv. Funct. Mater.*, 2019, **29**,
1–10.
- 40 J. H. Santos, M. T. J. Quimque, A. P. G. Macabeo, M. J. T.
Corpuz, Y. Wang, T. Lu, C. Lin and O. B. Villaflores,
Pharmaceutics, 2020, **12**, 437.
- 41 P. Horcajada, T. Chalati, C. Serre, B. Gillet, C. Sebrie, T.
Baati, J. F. Eubank, D. Heurtaux, P. Clayette, C. Kreuz, J.-S.
Chang, Y. K. Hwang, V. Marsaud, P.-N. Bories, L. Cynober, S.
Gil, G. Férey, P. Couvreur and R. Gref, *Nat. Mater.*, 2010, **9**,
172–178.
- 42 E. Bellido, M. Guillevic, T. Hidalgo, M. Santander-Ortega, C.
Serre and P. Horcajada, *Langmuir*, 2014, **100**, 5911–5920.
- 43 X. Li, L. Lachmanski, S. Safi, S. Sene, C. Serre, J. M.
Grenèche, J. Zhang and R. Gref, *Sci. Rep.*, 2017, **7**, 13142.
- 44 C. Tamames-Tabar, D. Cunha, E. Imbuluzqueta, F. Ragon, C.
Serre, M. J. Blanco-Prieto and P. Horcajada, *J. Mater.*
Chem. B, 2014, **2**, 262–271.
- 45 T. Baati, L. Njim, F. Neffati, A. Kerkeni, M. Bouttemi, R.
Gref, M. F. Najjar, A. Zakhama, P. Couvreur, C. Serre and P.
Horcajada, *Chem. Sci.*, 2013, **4**, 1597–1607.
- 46 T. Hidalgo, M. Giménez-Marqués, E. Bellido, J. Avila, M. C.
Asensio, F. Salles, M. V. Lozano, M. Guillevic, R. Simón-
Vázquez, A. González-Fernández, C. Serre, M. J. Alonso and
P. Horcajada, *Sci. Rep.*, 2017, **7**, 43099–43113.
- 47 E. Bellido, T. Hidalgo, M. V. Lozano, M. Guillevic, R. Simón-
Vázquez, M. J. Santander-Ortega, Á. González-Fernández,
C. Serre, M. J. Alonso and P. Horcajada, *Adv. Healthc.*
Mater., 2015, **4**, 1246–1257.
- 48 V. Agostoni, T. Chalati, P. Horcajada, H. Willaime, R. Anand,
N. Semiramoth, T. Baati, S. Hall, G. Maurin, H. Chacun, K.
Bouchemal, C. Martineau, F. Taulelle, P. Couvreur, C.
Rogez-Kreuz, P. Clayette, S. Monti, C. Serre and R. Gref,
Adv. Healthc. Mater., 2013, **2**, 1630–1637.
- 49 T. Chalati, P. Horcajada, P. Couvreur, C. Serre, M. Ben
Yahia, G. Maurin and R. Gref, *Nanomedicine*, 2011, **6**, 1–14.
- 50 S. Rojas, F. J. Carmona, C. R. Maldonado, E. Barea and J. A.
R. Navarro, *New J. Chem.*, 2016, **40**, 5690–5694.
- 51 U. E. P. Agency, *MSDS*, 2014.
- 52 A. García Márquez, A. Demessence, A. E. Platero-Prats, D.
Heurtaux, P. Horcajada, C. Serre, J.-S. Chang, G. Férey, V. A.
De La Peña-O’Shea, C. Boissière, D. Grosso and C. Sanchez,
Eur. J. Inorg. Chem., 2012, **100**, 5165–5174.
- 53 J. Zielonka, J. Gębicki and G. Grynkiewicz, *Free Radic. Biol.*
Med., 2003, **35**, 958–965.
- 54 J. A. Rothwell, A. J. Day and M. R. A. Morgan, *J. Agric. Food*
Chem., 2005, **53**, 4355–4360.
- 55 P. Horcajada, R. Gref, T. Baati, P. K. Allan, G. Maurin, P.
Couvreur, G. Férey, R. E. Morris and C. Serre, *Chem. Rev.*,
2012, **112**, 1232–1268.
- 56 R. A. King and D. B. Bursill, *Am. J. Clin. Nutr.*, 1998, **67**, 867–
872.

- 57 C. Tamames-Tabar, E. Imbuluzqueta, M. A. Campanero, P. Horcajada and M. J. Blanco-Prieto, *J. Chromatogr. B Anal. Technol. Biomed. Life Sci.*, 2013, **935**, 47–53.
- 58 S. Rojas, T. Baati, L. Njim, L. Manchego, F. Neffati, N. Abdejilil, S. Saguem, C. Serre, M. F. M. F. Najjar, A. Zakhama, P. Horcajada, N. Abdeljelil, S. Saguem, C. Serre, M. F. M. F. Najjar, A. Zakhama and P. Horcajada, *J. Am. Chem. Soc.*, 2018, **140**, 9581–9586.
- 59 M. Swartz and J. Smith, *bioRxiv*, 2019, 620898.
- 60 J. T. Kim, S. Barua, H. Kim, S. C. Hong, S. Y. Yoo, H. Jeon, Y. Cho, S. Gil, K. Oh and J. Lee, *Biomol. Ther.*, 2017, **25**, 452–459.